J. Indian Chem. Soc.,
Vol. 96, March 2019, pp. 335-348

Synthesis, characterization, DNA cleavage, docking and cytotoxic studies of novel nalidixic acid hydrazone and its Cu^{II}, Ni^{II} and Co^{II} complexes

Nagula Narsimha, Palreddy Ranjithreddy, Jaheer Mohmed, P. Sujitha and Ch. Sarala Devi*

Department of Chemistry, University College of Science, Osmania University, Hyderabad-500 007, Telangana, India

E-mail: dr_saraladevich@yahoo.com

Manuscript received online 19 March 2018, revised 23 July 2018, accepted 26 February 2019

Novel N′-(2-hydroxy-3-methoxy-benzylidene)-1-ethyl-1,4-dihydro-7-methyl-4-oxo-1,8-naphthyridine-3-carbohydrazide [NBNCH] and its solid metal complexes with Cu^{II}, Ni^{II} and Co^{II} were synthesized and characterized by employing spectro-analytical techniques viz. elemental analyses, magnetic susceptibilities measurements, ^{1}H NMR, UV-Vis, IR, Mass, TGA, SEM-EDX, ESR and spectrophotometry studies. The HyperChem 7.5 software was used for quantum mechanical calculations. The geometry optimization, contour maps of highest occupied molecular orbitals (HOMO) and lowest unoccupied molecular orbitals (LUMO) and corresponding binding energy values of molecular and ionic forms of title compound were computed using semi empirical single point PM3 method, in order to understand the binding modes of metal complexes. The stoichiometric studies of complexes determined spectrophotometrically using Job's continuous variation and mole ratio methods inferred 1:2 ratio in respective systems. The title compound and its metal complexes screened for antibacterial and antifungal properties indicated more pronounced activity of Cu^{II} complex compared to other compounds. The studies of nuclease activity for the cleavage of PBR322 DNA and MTT assay for *in vitro* cytotoxic properties showed high activity of Cu^{II} complex. The interaction studies of metal complexes with CT-DNA investigated by UV-Visible and fluorescence titrations revealed the intercalation mode of binding. Docking studies were also performed to illustrate the binding mode of the title compound with the target site of "Thymidine phosphorylase from *E. coli*" (PDB ID: 4EAF) protein.

Keywords: Quantum mechanical calculations, antifungal, docking, DNA interactions, cytotoxic studies.

Introduction

Quinolones are a group of antibiotics that have been abundantly used in treating several bacterial diseases[1]. Quinolones have been reported to have wide-ranging biological activities antitubercular[2], fungicidal[3], antimalarial, anticancer, anti-HIV agents[4], antiviral[5] and antibacterial activity[6]. Nalidixic acid (NA) was first synthetic quinolone derivative introduced for the treatment of urinary tract infection in 1963[7,8]. It is effective primarily against Gram-negative bacteria, with minor anti-Gram-positive activity. In lower concentrations, it exhibits bacteriostatic property and in higher concentrations it acts as bactericidal[9,10]. NA is also a very strong inhibitor of DNA replication in bacteria[11,12]. The hydrazides of NA have wide range of biological activities, namely antibacterial, antifungal[13,14], anticonvulsant[15], anti-inflammatory[16], antimalarial[17] and antituberculosis activities[18]. The corresponding hydrazone derivatives are used as active ingredients in the method for controlling agricultural and horticultural insect pests[19]. The metal complexes of 2-hydroxy-3-methoxybenzaldehyde have significant interest because of their pharmacological applications[20]. A survey of the literature reveals that no work has been carried out on the synthesis of complexes with hydrazones of nalidixic acid. So in the present study synthesis of nalidixic acid hydrazone viz. N'-(2-hydroxy-3-methoxybenzylidene)-1-ethyl-1,4-dihydro-7-methyl-4-oxo-1,8-naphthyridine-3-carbohydrazide [NBNCH] using 2-hydroxy-3-methoxybenzaldehyde is synthesized and characterized. The resultant title compound of present investigation and corresponding metal complexes were screened for antibacterial, antifungal and DNA cleavage studies. Further *in vitro* cytotoxic and their anticancer activities were evaluated. Docking studies were also planned with title compound to understand suitable active bind sites in 'Thymidine phosphorylase' protein.

Results and discussion

Characterization of NBNCH:

Mass spectrum:

The mass spectrum of the title ligand (NBNCH) exhibits (Fig. S1, Supplementary Information) peak at *m/z* 381 representing [M+1] peak. The spectrum also shows a peak at *m/z* 403 indicating expected sodium adduct. Elemental analyses (Found: C, 63.70; H, 5.10; N, 14.90. Calcd: C, 63.15; H, 5.30; N, 14.73%) indicated composition of title compound as $C_{20}H_{20}N_4O_4$.

^{1}H NMR and D_2O spectrum:

The ^{1}H NMR spectrum of NBNCH shows (Fig. S2, Supplementary Information) signals at δ 13.20 ppm (s, NH), 11.45 ppm (s, OH), 9.13 ppm (s, -CH=N-), 8.4 ppm (s, 1H, H-2-napthyridine), 8.65 ppm (d, 1H, H-5-napthyridine), 7.45 ppm (d, 1H, H-6-napthyridine) and 6.80–7.0 ppm (m, 3H, phenyl). The other signals were recorded δ 3.93 ppm (s, 1H, OCH_3), 4.63 ppm (q, 2H, N-CH_2), 1.53 ppm (t, 3H, N-CH_2 CH_3) and 2.72 ppm (s, 3H, 7-CH_3). The OH signal was identified by its disappearance in the D_2O exchange spectrum (Fig. S3, Supplementary Information).

IR spectrum:

IR spectrum of NBNCH displayed (Fig. S4, Supplementary Information) a broad band around 3240–3460 cm^{-1} which corresponds to phenolic ν(OH) and amide ν(N-H) stretching vibrations and the band at 3039 cm^{-1} represents ν(C-H aromatic) vibrations. The strong sharp bands appeared at 1687 cm^{-1}, 1612 cm^{-1} are characteristic stretching frequencies of ν(C=O) (Quinolone ring). The band at 1598 cm^{-1} is attributed to azomethine (C=N) vibrations and the band at 1193 cm^{-1} is ascribable to phenolic ν(C-O) vibration.

Electronic spectral data:

The electronic spectral data of NBNCH (Fig. S5, Supplementary Information) in DMSO shows absorption bands at 259 nm (38610 cm^{-1}) and 327 nm (30581 cm^{-1}) assignable to n→π* (C=O) and n→π* (C=N) transitions respectively.

Computational studies:

Quantum chemical calculations have been done employing HyperChem 7.5 software to analyze the donor and acceptor properties of title ligand in molecular and ionized forms[21]. The Eigen values of highest occupied molecular orbitals (E_{HOMO}) and lowest unoccupied molecular orbitals (E_{LUMO}) were computed with geometry optimized structure of NBNCH (Figs. 1(a) and 1(b)) using semi empirical single point PM3 method. The minus Eigen values correspond to binding energy values of electrons in corresponding orbitals. These values for frontier molecular orbitals (E_{HOMO} and E_{LUMO}) are important for the prediction of the reactivity of a species. The E_{HOMO} suggests the electron donating ability (Ionization energy) of a molecule and the E_{LUMO} is ability of a molecule to accept the electrons (Electron affinity). From the binding energy values it is clear that the energy difference in $E_{HOMO-LUMO}$ (Table 1) level is less in ionized form of NBNCH compared to its molecular form inferring high reactivity of former. The contour map of electrostatic potential suggests that the electron charge delocalization is more at electro negative atoms in both molecular and ionized forms of NBNCH.

Quantitative structure-activity relationship (QSAR):

Quantitative structure-activity relationship (QSAR) is a computational process that relates the chemical structure of compounds with biological activity. The QSAR parameters like surface area, hydration energy, log P, refractivity, polarisability and molecular properties were computed by

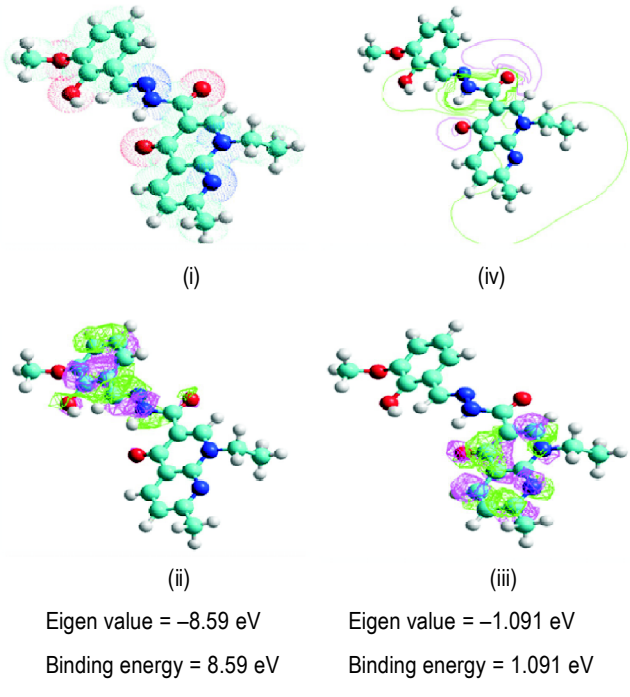

Fig. 1. (a) Molecular form of NBNCH: (i) Geometry optimized structure, (ii) Contour map of highest occupied molecular orbitals (HOMO), (iii) Contour map of lowest unoccupied molecular orbitals (LUMO) and (iv) Electrostatic potential contour map.

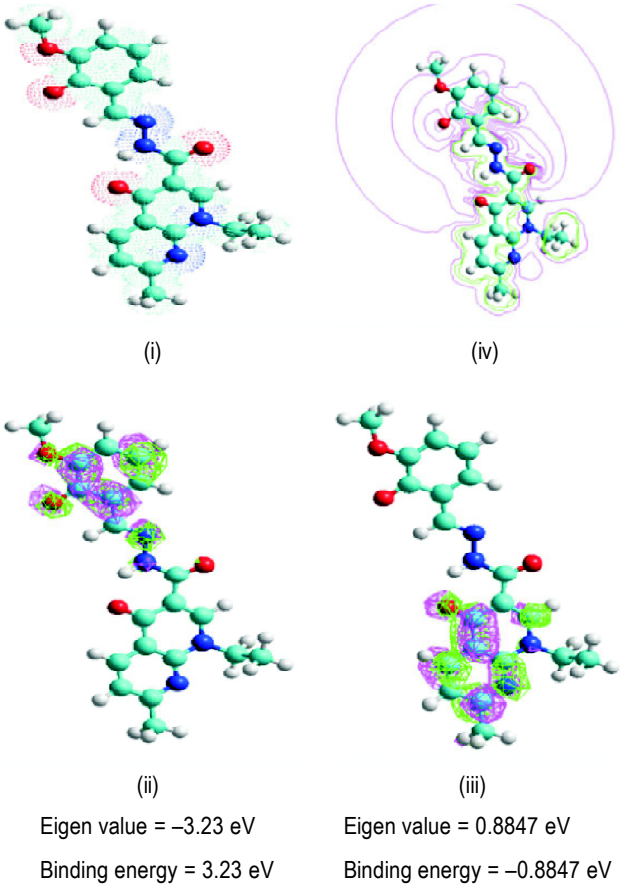

Fig. 1. (b) Ionized form of NBNCH: (i) Geometry optimized structure, (ii) Contour map of highest occupied molecular orbitals (HOMO), (iii) Contour map of lowest unoccupied molecular orbitals (LUMO) and (iv) Electrostatic potential contour map.

Table 1. The energy difference ($E_{LUMO-HOMO}$)

NBNCH	$E_{HOMO-LUMO}$ (eV)
Molecular form	7.499
Ionized form	4.1147

single point PM3 method. This analysis represents an attempt to relate structural descriptors of compounds with their physicochemical properties and biological activities. The log P value indicates the magnitude of lipophilicity character of NBNCH (Table 2).

Spectrophotometric studies:

The composition of metal complexes is determined by spectrophotometric studies using mole-ratio and Job's continuous variation methods.

Table 2. QSAR and molecular properties of NBNCH

QSAR properties:	
Surface Area (Approx.)	540.27 Å^2
Surface area (Grid)	649.98 Å^2
Volume	1096.71 Å^3
Hydration energy	–11.55 kcal/mol
log P	–0.10
Refractivity	109.88 Å^3
Polarizability	40.02 Å^3
Mass	380.40 amu
Molecular properties:	
Total energy	–103768.1094 kcal/mol
Dipole moment	4.371 Debyes
RMS gradient	0.1196 kcal/mol

Mole-ratio method:

Mole-ratio method is used to determine the metal to ligand ratio in Co^{II}-NBNCH system. The series of solutions are prepared wherein concentration of the metal ion is kept constant while the ligand concentration is varied. The pH of solutions is maintained constant by adding sodium acetate buffer and absorbance of each solution is measured at a wavelength (λ_{max}) 415 nm. The absorbance values increased until the stoichiometric amount ligand has been added to metal ion in equilibrating mixture. Once the stoichiometric amount of ligand is added further increment in absorbance is minimized. A graph plotted (Fig. 2) between absorbance and mole-ratio of the ligand inferred a point of intersection

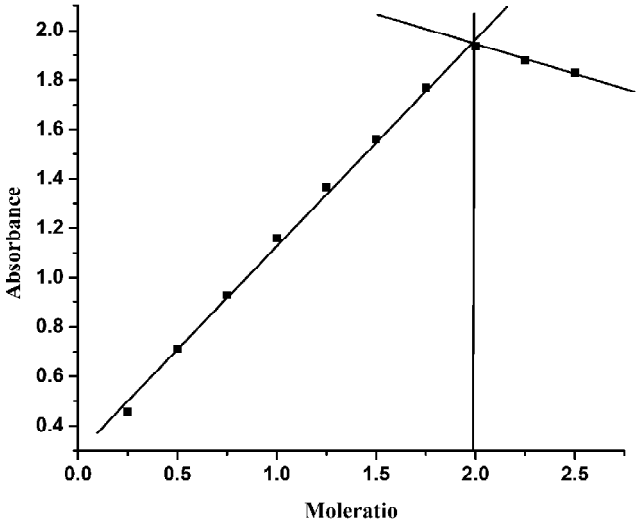

Fig. 2. Plot of absorbance versus mole ratio of ligand at 303 K in ethanol medium (Co^{II}-NBNCH (λ_{max} = 415 nm)).

corresponding to stoichiometric ratio of metal-ligand system understudy.

Job's continuous variation method:

Job's method involves mixing of equimolar solutions of metal and ligand (NBNCH) with different volume ratio and keeping total volume of the solution constant. The pH of solutions was maintained constant by adding sodium acetate buffer in the resulting mixture and absorbance of a series of mixtures is measured (λ_{max}) at 423 nm. The intersection point in the plot of mole fraction versus absorbance corresponds to 1:2 composition of complex (Fig. 3).

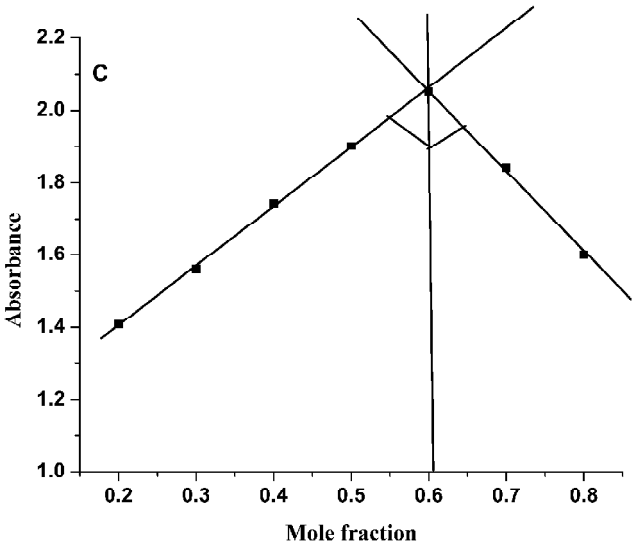

Fig. 3. Plot of absorbance versus mole ratio of ligand at 303 K in ethanol medium (Cu^{II}-NBNCH (λ_{max} = 423 nm)).

Characterization of NBNCH metal complexes:

Mass and elemental analyses:

The mass spectrum of Cu^{II}-NBNCH displayed (Fig. S6, Supplementary Information) a less intensity peak at *m/z* 844.3 corresponding to [M+Na] peak. The mass of molecular ion calculated from this sodium adduct peak represents 1:2 composition (M:2L) of metal complex.

The mass spectrum of Co^{II}-NBNCH (Fig. S7, Supplementary Information) displayed peak at *m/z* 817.3 corresponding to 1:2 metal to ligand composition(M:2L) in metal complex.

The mass spectrum of Ni^{II}-NBNCH showed (Fig. S8, Supplementary Information) peak at *m/z* 817.3 corresponding to the molecular ion peak, which indicates the formation of metal complex in 1:2 mole ratio (M:2L). The results obtained from elemental analyses presented in Table 3, showed metal to ligand ratio as 1:2 ($M:L_2$) in all the aforementioned complexes.

IR spectra:

IR spectra give sufficient information to understand modes of bonding in any compound with potential donor sites. In the present investigation the IR spectrum of the NBNCH is compared with the IR spectra of its metal complexes (Figs. S9–S11, Supplementary Information). The IR spectra of Cu^{II}, Ni^{II} and Co^{II} complexes showed a broad band around 3419–3531 cm^{-1} indicating the presence of coordinated water molecules in corresponding systems, which is further augmented by TGA/DTA analyses of the complexes. In all metal complexes the stretching frequency of phenolic ν(OH) disappeared and also the phenolic ν(C-O) band is shifted to lower frequency from 1193 cm^{-1} to 1150–1170 cm^{-1} in the range, indicating the participation of phenolic oxygen in bonding with metal ions understudy. The stretching frequency of azomethine ν(C=N) vibration band also is shifted to lower frequency[22] from 1598 cm^{-1} to in the range of 1533 cm^{-1}–1537 cm^{-1} in all respective metal complexes inferring the coordination of azomethine nitrogen. The presence of metal-ligand bonds is further confirmed by the appearance of two new bands in far IR region at 425–500 cm^{-1} and 550–575

Table 3. Elemental analyses and physical properties of NBNCH metal complexes

Empirical formula	Yield (%)	Colour	Analyses: Found (Calcd.) (%) C	H	N	Metal	Λ (Ω^{-1} cm^2 mol^{-1})
$Cu(C_{20}H_{19}N_4O_4)_2.2H_2O$	80	Forest green	54.96 (55.97)	4.90 (4.93)	13.07 (13.05)	6.90 (7.40)	14
$Ni(C_{20}H_{19}N_4O_4)_2.2H_2O$	62	Mustard	57.35 (56.27)	4.94 (4.96)	13.34 (13.12)	6.94 (6.90)	12
$Co(C_{20}H_{19}N_4O_4)_2.2H_2O$	75	Maroon	55.30 (56.29)	4.93 (4.96)	13.18 (13.13)	6.90 (6.88)	13

cm^{-1} [23] assignable to ν(M-N) and ν(M-O) bands respectively.

Electronic spectral data:

When, the electronic spectrum of title compound is compared with the electronic spectra of its metal complexes (Fig. 4), the appearance of new absorption bands at 419 nm (23866.35 cm^{-1}), 437 nm (22883.30 cm^{-1}) and 425 nm (23529.41 cm^{-1}) ascribable to d-d transitions are observed in Cu^{II}, Ni^{II} and Co^{II} complexes respectively.

SEM and EDX:

SEM (Scanning Electron Microscope) can be utilized for high magnification imaging of almost all materials. With SEM in combination with EDX (Energy Dispersive X-ray Spectroscope) it is also possible to find out elemental composition of a sample. Scanning electron microscopy is used to evaluate morphology and particle size of the NBNCH and its metal complexes (Figs. S12–S15, Supplementary Information). It is seen from the figures that the NBNCH shows flake like morphology with 200 nm partial size. In Cu^{II}, Ni^{II} and Co^{II} complexes distinct morphologies are observed with 200 nm, 200 nm and 2 nm particle size respectively. The chemical composition of the title compound and its metal complexes determined with EDX analyses is in good agreement with the mass spectral results in corresponding systems.

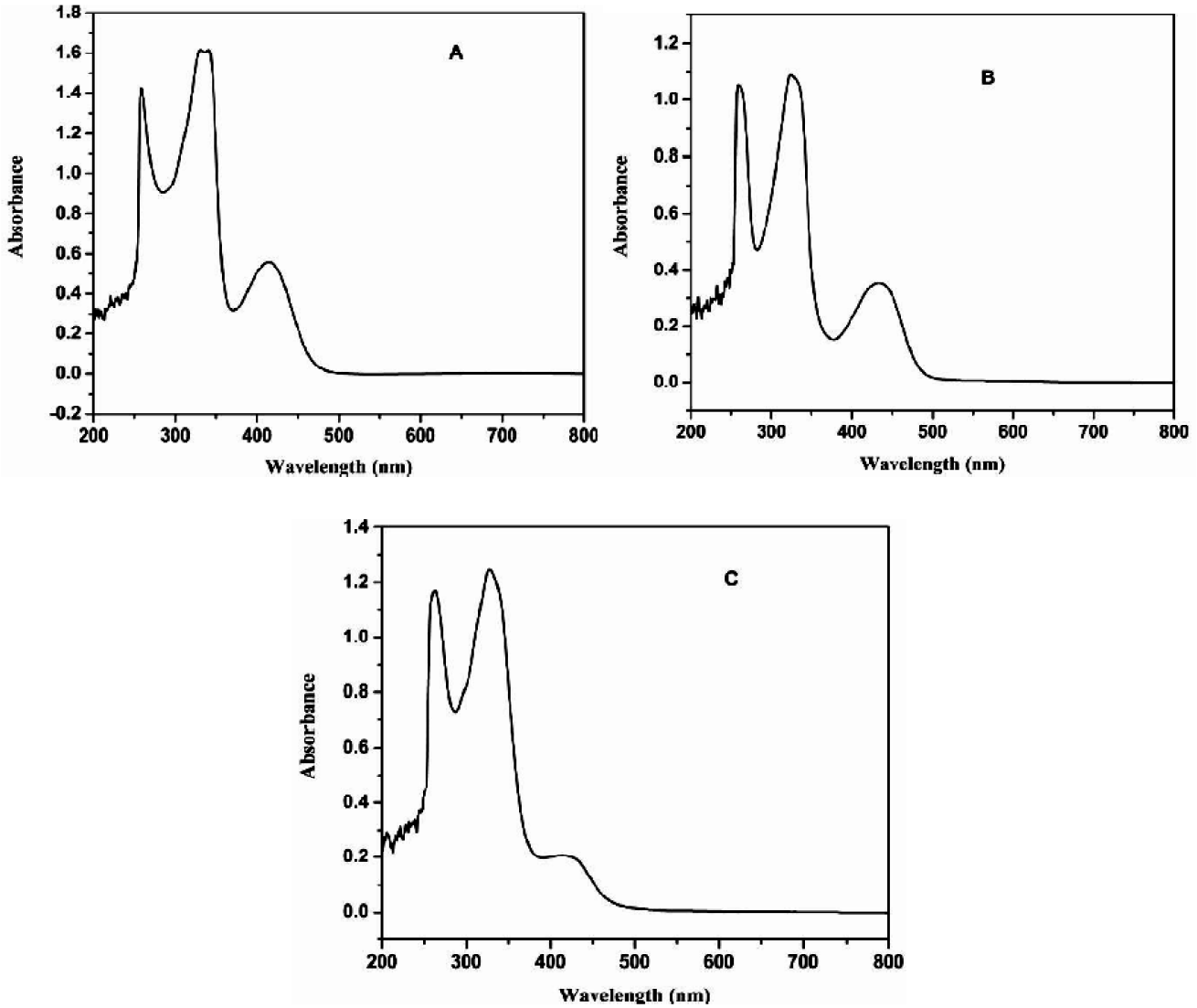

Fig. 4. UV-Vis spectrum of (A) Cu^{II}-NBNCH, (B) Ni^{II}-NBNCH and (C) Co^{II}-NBNCH.

Thermal analysis:

In the present investigation, the thermal stability and degradation behavior of Cu^{II} and Co^{II} metal complexes are studied by TGA-DTA under nitrogen atmosphere.

Thermogram of Cu^{II}-NBNCH presented in Fig. S16 (Supplementary Information) showed initial weight loss in the temperature range 160–260°C accompanied by energy absorption evident from endothermic peak at 183°C in DTA curve indicating loss of coordinated water molecules. The second weight loss appeared in the temperature region 272–518°C and an endothermic peak at 510°C in DTA corresponds to the decomposition of ligand. Further weight loss in the temperature range 518–910°C corresponding to continuous sublimation of ligand moiety and an exothermic peak at 590°C in DTA curve represent pyrolytic nature due to more number of nitrogen atoms present in ligand moiety. Above this temperature a slight increase in the weight of residue indicates formation of an air stable metal oxide.

Thermogram of Co^{II}-NBNCH metal complex showed (Fig. S17, Supplementary Information) weight loss in three stages. The steep slow stage in the temperature 259.4°C and an endothermic peak at 190°C in DTA corresponding to the loss of coordinated water molecules. In the temperature region of 259.4–803°C and an exothermic peak at 563°C in DTA the decomposition of total ligand moiety and above this temperature remaining residue is stable metal oxide.

ESR spectrum:

The ESR spectrum of Cu^{II}-NBNCH metal complex at 77 K (liquid nitrogen temperature) is presented in Fig. 5. The Cu^{II} complex exhibited the $g_{||}$ value of 2.086 and $g_{\perp}$ value of 2.041. The trend $g_{||} > g_{\perp}$ suggests axially elongated octahedral geometry and presence of unpaired electron in $d_{x^2-y^2}$ orbital[24]. The spectrum further showed four hyperfine peaks in $g_{||}$ region as a result of electron spin interaction with nuclear spin of copper ($^{63}Cu = 3/2$) and are attributable to transitions $+3/2 \rightarrow +3/2$, $+1/2 \rightarrow +1/2$, $-1/2 \rightarrow -1/2$ and $-3/2 \rightarrow -3/2$ within m_I levels based on selection rules ($\Delta m_s = \pm 1$ and $\Delta m_I = 0$).

Magnetic susceptibilities measurements:

The calculated magnetic moments of Cu^{II}-NBNCH, Ni^{II}-NBNCH and Co^{II}-NBNCH complexes are 1.92, 2.78 and 3.88 B.M. respectively. This reveals the paramagnetic behavior

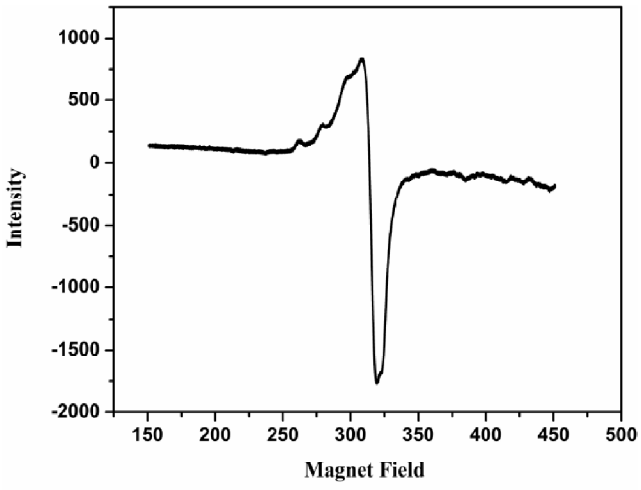

Fig. 5. ESR spectrum of Cu^{II}-NBNCH at 77 K.

of all complexes. Based on the above interpretation the following tentative structures are assigned for the complexes (Fig. 6).

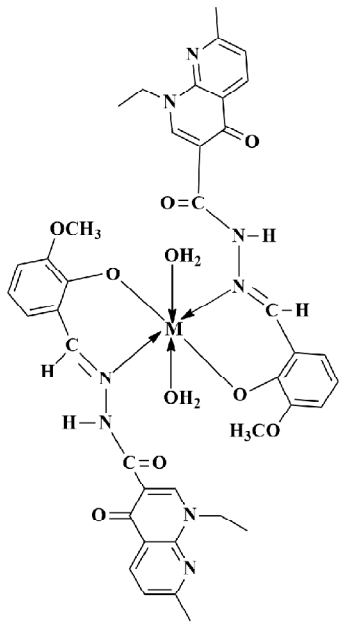

Fig. 6. Tentative structure of NBNCH complex. M: Cu^{II}, Ni^{II} and Co^{II}.

Biological studies:

DNA cleavage studies:

The cleavage activity of NBNCH and its Cu^{II}, Ni^{II} and Co^{II} complexes has been carried out by agarose gel electrophoresis method using supercoild plasmid PBR322 DNA as a substrate. The experiment (Fig. 7) clearly revealed that

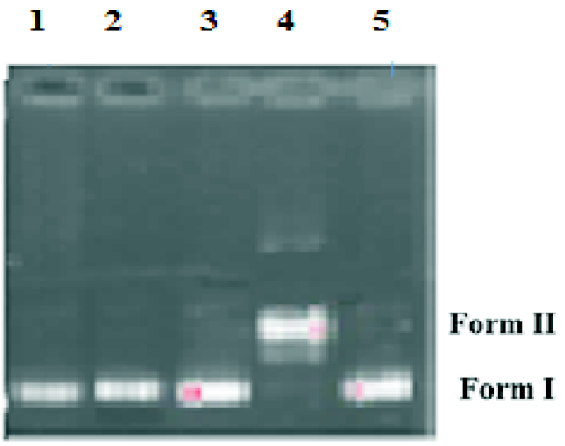

Fig. 7. DNA cleavage studies on NBNCH, Cu^{II}-NBNCH, Co^{II}-NBNCH and Ni^{II}-NBNCH. Lane 1: DNA marker (1 μL + 4 μL Tris-HCl buffer); Lane 2: DNA (1 μL + 4 μL Tris-HCl buffer) + Ni^{II} (5 μL of 2 mg/ml); Lane 3: DNA (1 μL + 4 μL Tris-HCl buffer) + Co^{II} (5 μL of 2 mg/ml); Lane 4: DNA (1 μL + 4 μL Tris-HCl buffer) + Cu^{II} (5 μL of 2 mg/ml); Lane 5: DNA (1 μL + 4 μL Tris-HCl buffer) + NBNCH (5 μL of 2 mg/ml).

Cu^{II} complex is found to be most efficient cleaver which has converted supercoild DNA (form I) into relaxed DNA (form II). Whereas other compounds have not exhibited any apparent cleavage. From these results we deduce that Cu^{II} complex acts as a potent nuclease agent.

Antibacterial activity:

NBNCH and its metal complexes are screened for their *in vitro* antibacterial activity against *Bacillus*, *Escherichia coli*, *Staphylococcus* and *Pseudomonas* bacteria (Fig. S18, Supplementary Information) using Streptomycin as standard. As the solutions are prepared in DMSO medium, the activity due to solvent is also evaluated (Fig. S19, Supplementary Information).

Antibacterial activity was tested by standard agar diffusion method. Fresh bacterial culture having 5×10^{-5} colonies is mixed with nutrient agar medium and poured into plates. 100 μL of each compound dissolved in DMSO (500 μg/ml) is loaded in the well. The activity or sensitivity was observed after 24–48 h incubation at 37°C. The zone of inhibition was recorded in centimeters as shown in Table 4. The biological activity of the title compound and its metal complexes revealed the potential biological activity of all compounds under investigation. However copper complex showed relatively higher activity.

Antifungal activity:

Antifungal activity studies were carried out using two fungi. Potato dextrose agar medium was prepared and the fungal plugs were placed in the center of the plate and the compounds were put in the wells surrounding the plug and the results were collected after 72 h.

Antifungal activity studies of the NBNCH and its complexes were tested against two fungi species namely *Sclerotium rolfsii* and *Macrophomina phaseolina*, cultured on potato dextrose agar medium. Indofil fungicide is used in the technique as the standard antifungal agent. In this, potato dextrose agar media was prepared and the fungal plugs were placed in the center of the plate and the compounds were put in the wells surrounding the plug and the results were collected after 72 h. The results of the antifungal activities are given in Table 5. The results show that all compounds exhibit (Fig. S20, Supplementary Information) higher antifungal activity against all organisms than standard antifungal agent. The higher activity of the metal complexes may be due to the effect of metal ions on the normal cell membrane. The importance of this lies in the fact that, these compounds could be applied fairly in the treatment of some common diseases caused by *Sclerotium rolfsii* and *Macrophomina phaseolina*.

Table 4. Zone of inhibition of NBNCH and its metal complexes against four different bacteria

Sr. No.	Compd.	*Bacillus* (cm)	*Escherichia coli* (cm)	*Staphylococcus* (cm)	*Pseudomonas* (cm)
1.	NBNCH	1.4	1.3	–	1.2
2.	Cu^{II}-NBNCH	1.6	1.5	1.2	1.2
3.	Ni^{II}-NBNCH	1.5	1.4	–	1.2
4.	Co^{II}-NBNCH	1.5	1.3	–	1.2
5.	Streptomycin (standard)	2.4	2.0	3.6	2.0
6.	DMSO	–	–	–	–

Table 5. Zone of inhibition of NBNCH and its complexes against two different fungi

Sr. No.	Compound	Sclerotium rolfsii (cm)	Macrophomina phaseolina (cm)
1.	NBNCH	2.2	2.0
2.	Cu^{II}-NBNCH	2.3	2.1
3.	NI^{II}-NBNCH	2.1	2.0
4.	Co^{II}-NBNCH	2.2	2.1
5.	Indofil (standard)	2.0	1.6

In vitro cytotoxicity studies:

The cytotoxicity effect of NBNCH and its complexes is carried out using a standard MTT assay.

Protocol-cytotoxicity:

The HeLa (Cervical cancer) cell lines are cultured in DMEM medium which is supplemented with 10% heat inactivated fetal calf serum (FBS) and 1% Antibiotic-Antimycotic 100X solution.

(i) The cells are seeded at a density of approximately 5×10^3 cells/well in a 96-well flat-bottom micro plate and maintained at 37°C in 95% humidity and 5% CO_2 for overnight.

(ii) Each sample in various concentrations (100, 50, 25, 12.5, 6.25 µg/300 ml) is treated with cells taken in wells. Then cells were incubated for another 48 h.

(iii) The cells in well are washed twice with phosphate buffer solution, and 20 µL of the MTT staining solution (5 mg/ml in phosphate buffer solution) is added to each well and then incubated at 37°C.

(iv) After 4 h, 100 µL of dimethyl sulfoxide (DMSO) is added to each well to dissolve the formazan crystals and absorbance is recorded at 570 nm using micro plate reader.

(v) Formula: Surviving cells (%) = Mean OD of test compound/Mean OD of negative control×100

Inhibiting cells (%) =100 – Surviving cells

(vi) Using graph Pad Prism Version5.1, the IC_{50} values of enzyme are calculated.

Results

The cytotoxicity of compounds NBNCH and its metal complexes is evaluated against HeLa (Cervical cancer) cell lines. The results reveal that as concentration of the compounds increases the percentage of cell viability decreases (Fig. 8(a), Table S1 (Supplementary Information)). The microscopic images (Fig. 8(b)) revealed morphological changes in cells on treatment with compounds. The IC_{50} values (IC_{50} value is the concentration required to diminish the cell population growth by 50%) (Table 6) derived from *in vitro* screening studies revealed that Cu^{II} complex exhibits more anti-proliferative activity than NBNCH and other complexes. The results of present investigation predict the order of antitumor activity as Cu^{II}-NBNCH > Co^{II}-NBNCH > Ni^{II}-NBNCH > NBNCH. Such an observation may be attributed to the extended planar structure induced by the p→π* conjugation resulting from the chelation of ligand with the metal ion.

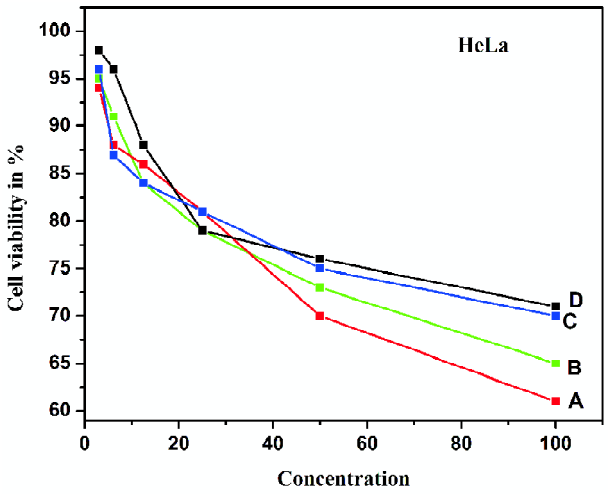

Fig. 8(a). Effect of concentration (3.062–100 µg) of A: Cu^{II}, B: Co^{II}, C: Ni^{II} and D: NBNCH on viability of HeLa (Cervical cancer) cell lines.

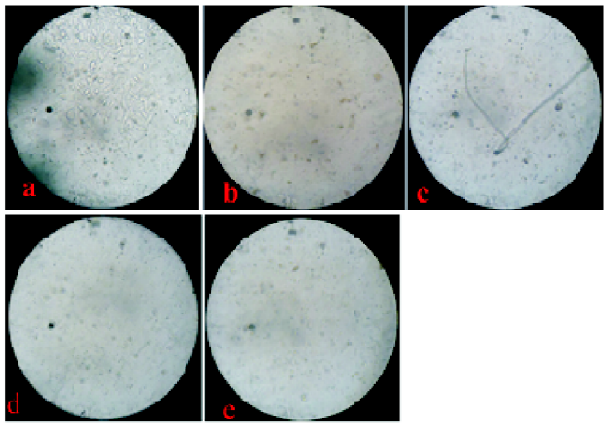

Fig. 8(b). Morphological changes in HeLa (Cervical cancer) cell incubated for 48 h: (a) control, (b) NBNCH, (c) Cu^{II} (d) Co^{II} and (e) Ni^{II}.

Table 6. The IC_{50} values for NBNCH and its complexes against HeLa cell line

Compound	IC_{50} (μM)
NBNCH	2.48
Cu^{II}-NBNCH	1.39
Ni^{II}-NBNCH	2.33
Co^{II}-NBNCH	1.75
Paclitaxel	0.3

DNA binding studies:

Absorption studies:

Absorption studies were recorded on a Shimadzu 2600 UV-Visible spectrophotometer. Absorption titration experiments were performed with fixed concentration of the metal complex (5 μM) and varying the concentration of CT-DNA (0–5 μM). Each time solutions were mixed for 5 min prior to recording their absorption spectra. The titration was continued until there was no change in absorbance which infers saturation point for binding. For Cu^{II}, Ni^{II} and Co^{II} complexes of title compounds, the binding constants (K_b) were determined from the spectroscopic titration data using the following equation[25].

$$[DNA]/(\varepsilon_a - \varepsilon_f) = [DNA]/(\varepsilon_b - \varepsilon_f) + 1/K_b\,(\varepsilon_b - \varepsilon_f) \text{ (Wolfe-Shimer equation)} \quad (1)$$

The apparent absorption coefficient ε_a, correspond to A_{obs}/[metal complex] in absence of DNA. In presence of DNA the terms ε_f and ε_b correspond to the extinction coefficient of the free metal complex (unbound) and the fully bound metal complex to DNA respectively.

Fluorescence studies:

To further support the binding studies of metal complexes, the interaction pattern between the metal complexes and CT-DNA was studied with ethidium bromide (EB) bound to CT-DNA solution in Tris buffer (5 mM Tris-HCl, 50 mM NaCl, pH 7.2) using fluorescence spectrophotometer. In the present investigation fluorescence study was performed on a JASCO FP-8500 spectrofluorometer. Titrations were performed by keeping the concentration of the EB (36 μM), DNA (36 μM) constant and by varying complex concentration 0–36 μM. The relative binding affinity of the metal complexes with CT-DNA was determined by measuring the quenching constant (K_{sv}) from the Stern-Volmer equation[26].

$$I_0/I = K_{sv}[r] + 1 \text{ (Stern-Volmer equation)} \quad (2)$$

where I_0 and I represent the fluorescence intensities in the absence and presence of the quencher, respectively. K_{sv} is a linear Stern-Volmer quenching constant and [r] is the quencher concentration. The quenching constant (K_{sv}) can be obtained using the plot of (I_0/I) versus [r].

For a static quenching interaction, the fluorescence intensity data can also be used to determine the apparent binding constant (K_b) and the number of binding sites (n) for the complex by the following equation[27].

$$\log [F_0 - F/F] = \log K_b + n \log [Q] \text{ (Scatchard equation)} \quad (3)$$

From the plot of log [($F_0 - F/F$)] versus log [Q], binding stoichiometry (n) has been obtained from slope and binding constant (K_b) from intercept value.

The changes in the absorption spectra of the Cu^{II}-NBNCH, Ni^{II}-NBNCH and Co^{II}-NBNCH complexes at a constant concentration prior to and after the addition of CT-DNA in small increments is shown in Fig. 9(a). Upon the addition of increasing amount of CT-DNA for a fixed concentration of complexes, the peak positions in complexes were altered, resulting in the distinguished hypochromic shift with a slight bathochromic shift. The hypochromism and bathochromism are ascribable to intercalative mode of binding involving a stacking interaction between the aromatic chromophores of the intercalated complexes and the base pairs of DNA duplex[28].

In order to compare quantitatively the binding strength of the complexes, the intrinsic binding constants K_b of the complexes with DNA were obtained by monitoring the changes in absorbance at 327 nm for Cu^{II}, 326 nm for Ni^{II} and 335 nm for Co^{II} with increasing concentration of DNA using Wolfe-Shimer equation.

The calculated binding constant (K_b) values of Cu^{II}, Ni^{II} and Co^{II} complexes are presented in Table 7. These results indicate that the binding affinity of all metal complexes with CT-DNA is moderate in comparison with strong intercalators. However the DNA binding affinities of these complexes follow the order: Cu^{II}-NBNCH > Co^{II}-NBNCH > Ni^{II}-NBNCH.

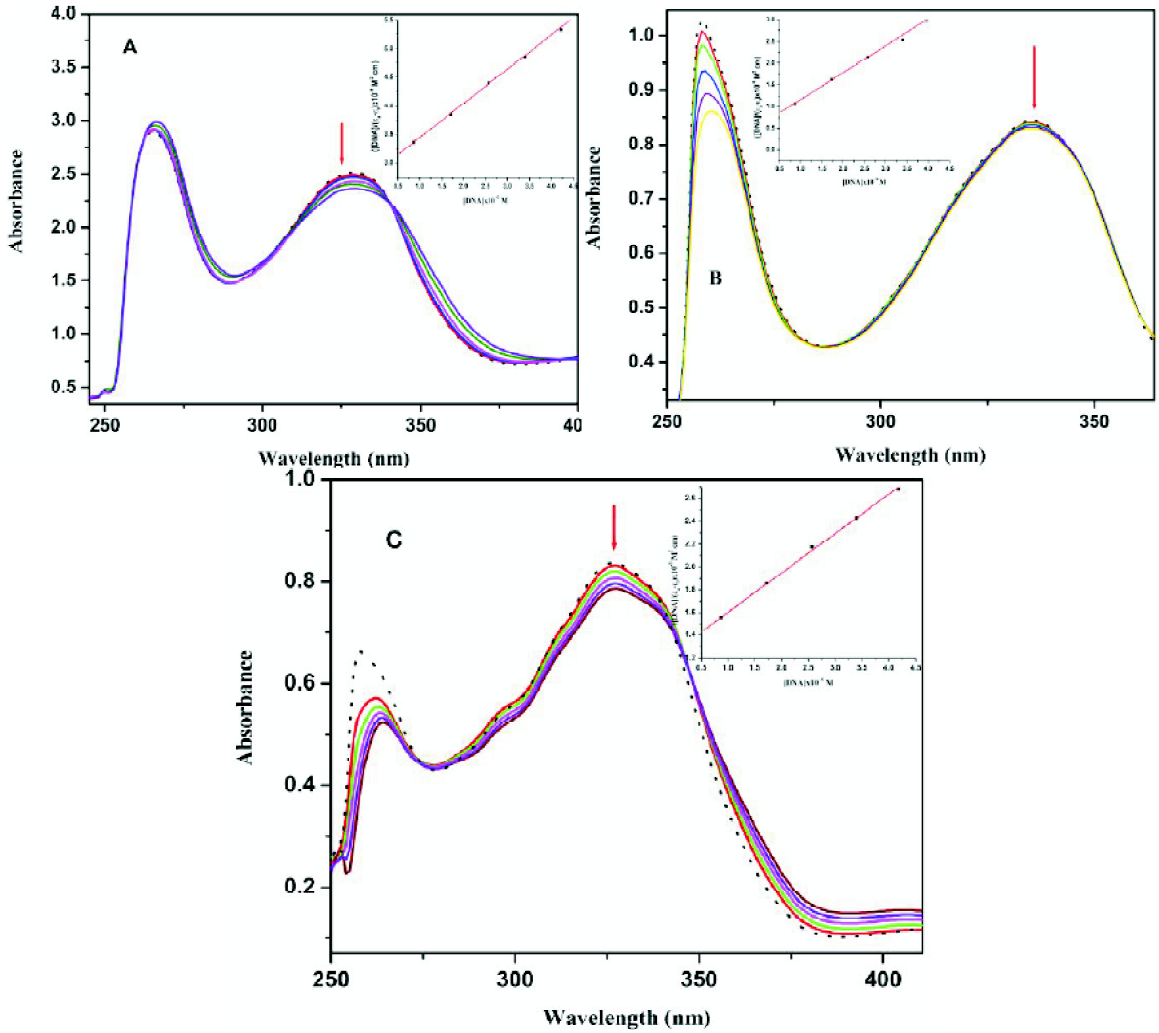

Fig. 9(a). Absorption spectra of complexes (A) Cu^{II}-NBNCH, (B) Co^{II}-NBNCH, (C) Ni^{II}-NBNCH in the absence (dotted line) and presence (solid lines) of increasing concentrations of CT-DNA in Tris-HCl buffer. Arrow shows the hypochromic and bathochromic shift upon increase of the DNA concentration. Inset: linear plot for the calculation of the intrinsic binding constant, K_b for DNA binding.

On addition of complexes Cu^{II}-NBNCH, Ni^{II}-NBNCH and Co^{II}-NBNCH to CT-DNA pretreated with EB a significant reduction in the emission intensity (Fig. 9(b)) was observed, indicating competitive intercalation of complexes and thus effecting the equilibrium for the formation of [DNA-EB] complex. The classical Stern-Volmer constant (K_{sv}), binding constant (K_b) values and number of binding sites (n) of the metal complexes estimated using eqs. (2) and (3) are in the order of Cu^{II}-NBNCH > Co^{II}-NBNCH > Ni^{II}-NBNCH. The comparison (Table 7) of K_b values estimated by both absorption and fluorescence titrations are in good agreement[29].

Docking studies:

Auto Dock software is employed to carry out molecular docking studies. Docking enables in understanding the molecular interactions between a compound and corresponding receptor[30]. In the present investigation molecular docking studies were carried out to understand the binding mode of NBNCH against "Thymidine phosphorylase from *E. coli*" (PDB ID: 4EAF) protein (Fig. 10). For docking, the protein structure (PDB ID: 4EAF) is detached from the inhibitor and hydrogen atoms were added. The binding free energy, hydrogen bond and RMSD were used to determine the binding

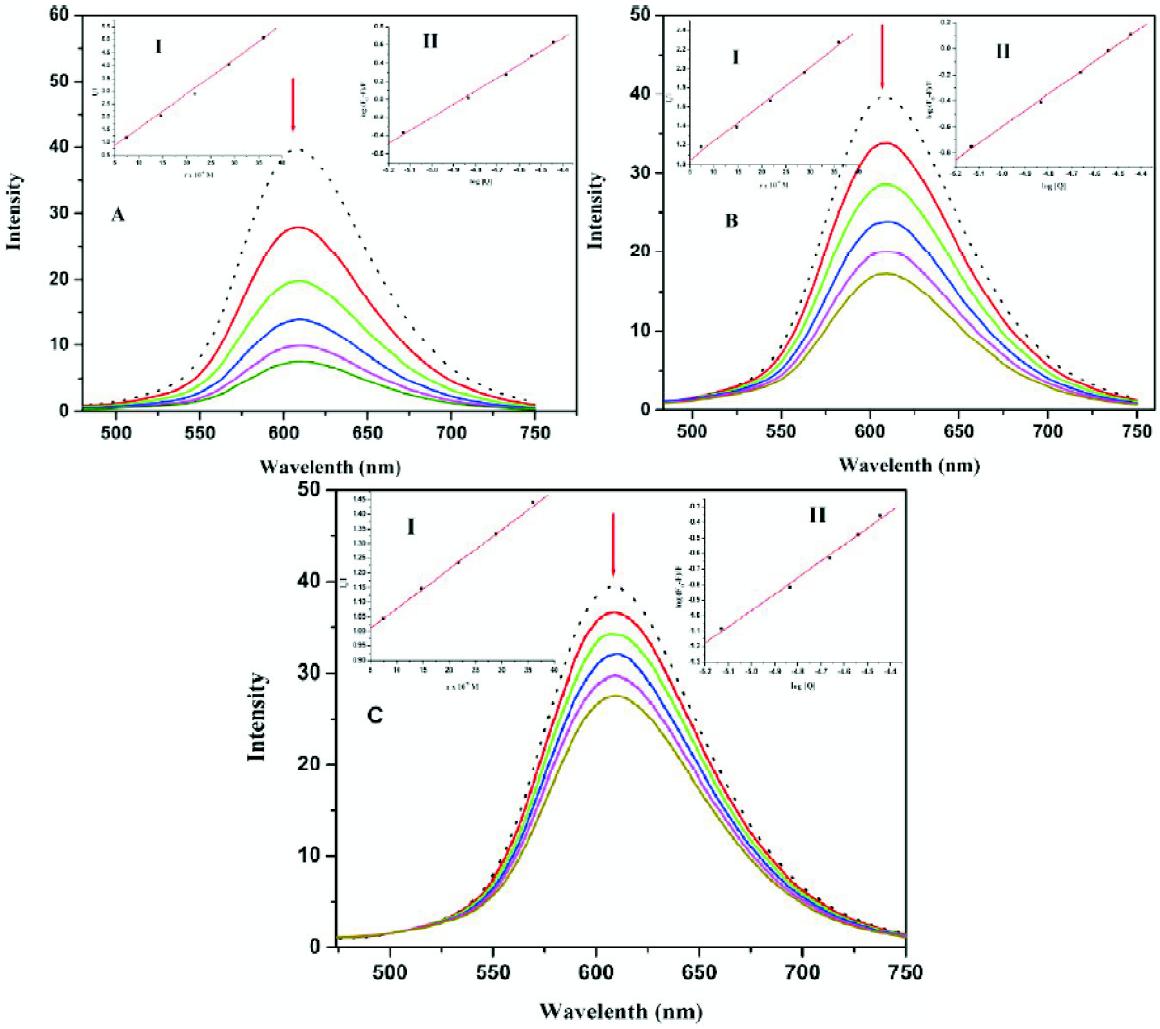

Fig. 9(b). Emission spectra of the DNA-Ethidium Bromide (EB) with (A) Cu^{II}-NBNCH, (B) Co^{II}-NBNCH, (C) Ni^{II}-NBNCH, arrows show the emission intensity changes upon increasing concentration of the compounds. Insert: Stern-Volmer equation plots (I), Scatchard equation plots (II).

Table 7. DNA binding studies of NBNCH metal complexes

	CT-DNA					
	Absorption binding		Emission quenching			
Complex	K_b	log K_b	K_b	log K_b	K_{sv}	n
Cu^{II}-NBNCH	$2.10\pm0.01\times10^5$ M^{-1}	5.32	$5.0\pm0.02\times10^5$ M^{-1}	5.70	$3.80\pm0.02\times10^5$ M^{-1}	1.45
Co^{II}-NBNCH	$1.62\pm0.02\times10^5$ M^{-1}	5.20	$2.0\pm 0.02\times10^5$ M^{-1}	5.30	$1.33\pm0.001\times10^5$ M^{-1}	1.26
Ni^{II}-NBNCH	$1.35\pm0.01\times10^5$ M^{-1}	5.13	$1.2\pm0.01\times10^5$ M^{-1}	5.07	$1.23\pm0.001\times10^4$ M^{-1}	1.05

affinity. Results obtained from Auto Dock provided pertinent information on the binding orientation of ligand-receptor interactions. The free energy of binding (ΔGb) calculated by Auto Dock programme is presented in Table 8.

Docking results:

Molecular Docking was accomplished using Auto Dock 4.2 which is used to predict the affinity, activity and binding orientation of NBNCH on the target protein "Thymidine

phosphorylase from *E. coli*". Binding analysis was based on free energy of binding, lowest docked energy and calculated RMSD values. NBNCH was found to bind at active site of 4EAF with lowest binding energy of –7.03 kcal/mol. Docking analysis of 4EAF with NBNCH enabled us to identify specific residues viz. Gln156, Lys190 within 4EAF. As the lower binding energy value indicates more thermodynamically favored interactions it infers that host pocket has suitable receptor sites to bind the title compound.

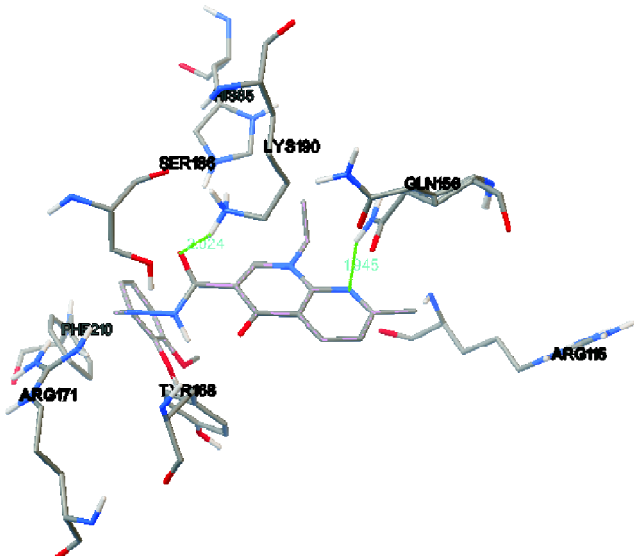

Fig. 10. Interaction of NBNCH with "Thymidine phosphorylase from *E. coli*" (colored by atom: carbon – grey; nitrogen – blue; oxygen – red) hydrogen bonds are indicated as green lines.

Table 8. Docking interactions of title compound and their binding energy value

Name of the compound	Name of the source protein	Interacting amino acids	Grid X-Y-Z coordinates	Free energy ΔG (kcal/mol)
NBNCH	4EAF	Gln156, Lys190	36.678, –8.372, 2.769	–7.03

Conclusions

Novel hydrazone NBNCH and its Cu^{II}, Ni^{II} and Co^{II} metal complexes are characterised by various physico-chemical techniques viz. elemental analysis, ^{1}H NMR, UV-Vis, IR, Mass, TGA, SEM-EDX and ESR and magnetic susceptibilities measurements. The results of antibacterial and antifungal revealed that all the synthesized compounds have shown good activity. DNA interaction studies with synthesized compounds by agarose gel electrophoresis method showed that DNA hydrolytic cleavage is more pronounced in presence of Cu^{II} metal complex. The results of *in vitro* cytotoxic screening of synthesized compounds revealed that all the compounds show remarkable cytotoxicity against HeLa cancer cell lines, wherein Cu^{II} have enhanced cytotoxic activity than other compounds. DNA binding studies by absorption titration method showed hypochromism and a red shift, due to the intercalation mode of binding involving strong stacking interactions between an aromatic chromophore of ligand moiety in corresponding complexes and the base pairs of DNA. The fluorescence reducing curve of EB-bound CT-DNA by complexes is in good agreement with the classical Stern-Volmer and Scatchard equation. The results both from electron absorption and fluorescence quenching revealed that the binding affinities of the complexes with CT-DNA are in the order of Cu^{II}-NBNCH > Co^{II}-NBNCH > Ni^{II}-NBNCH. Docking studies revealed potential binding of title compound with Thymidine phosphorylase protein target site.

Experimental

Instruments:

The mass spectral data were obtained employing electrospray ionization method (ESI-MS) and IR spectra were recorded (200–4000 cm^{-1}) on Perkin-Elmer 337 spectrophotometer in KBr pellet, while the electronic absorption spectra were recorded on Shimadzu UV spectrophotometer in the wavelength range of 200–800 nm. Spectrophotometry studies were performed on ELICO SL 177 instrument. ^{1}H NMR spectrum of title compound was obtained in $CDCl_3$ solution on a Bruker WH (270 MHz) instrument. Thermal analyses were carried out using Shimadzu TGA-50H in nitrogen atmosphere; SEM images were recorded in INCA EDX analyzer. The elemental analyses of compounds under study were carried out on atomic absorption spectrophotometer (ELICO-SL 163). ESR spectra were scanned on JES - FA200 ESR Spectrometer with X band at 77 K (liquid nitrogen temperature). Melting points were determined in Polmon apparatus (Model No. MP-90). Magnetic properties of metal complexes have been determined on a Gouy balance model 7550 at room temperature using $Hg[Co(SCN)_4]$ as standard. Fluorescence studies were performed on a JASCO FP-8500 spectrofluorimeter. The computational studies were carried out by using HyperChem 7.5 software. The DNA cleavage

activities were monitored using agarose gel electrophoresis. Docking studies were carried out by using Autodock 4.2 software.

Synthesis:

N′-(2-Hyroxy-3-methoxybenzylidene)-1-ethyle-1,4-dihydro-7-methyl-4-oxo-1,8-naphthyridine-3-carbohydrazide (NBNCH) synthesis involves in three steps.

Step-I: Synthesis of nalidixic acid ester (Methyl 1-ethyl-1,4-dihydro-7-methyl-4-oxo-1,8-naphthyridine-3-carboxylate):

Nalidixic acid (2 g, 8.611 mmol) and tetrahydro furan (60 ml) were placed in a 250 ml round bottom flask and mounted over a magnetic stirrer. Anhydrous potassium carbonate (5.96 g, 43.05 mmol) was added and the contents were stirred for one hour. Dimethyl sulfate (1.65 ml, 12.92 mmol) was added to this stirred solution and the mixture was refluxed at 70°–80°C. The progress of the reaction was monitored by TLC using hexane/ethyl acetate (80:20) as the eluent. After 5 h the new spot is observed on TLC plate. After the completion of reaction the solvent was removed under reduced pressure on a rotary evaporator and the product was extracted with chloroform. The chloroform layer was dried over anhydrous sodium sulfate and concentrated under reduced pressure to give the desired ester.

Step-II: Synthesis of nalidixic acid hydrazide (1-ethyl-1, 4-dihydro-7-methyl-4-oxo-1,8-naphthyridine-3-carbohydrazide):

The above synthesized ester (2 g, 8.17 mmol) was dissolved in tetrahydro furan (60 ml) in a 250 ml round bottom flask and $NH_2NH_2.H_2O$ (0.9 ml) was added. The contents were refluxed for 3 h. To the resultant reaction mixture, cold water (60 ml) was added and stirred for 20 min. A solid separated out was filtered at pump and dried.

Step-III: Synthesis of Nalidixic acid hydrazone (NBNCH):

The above prepared hydrazide (0.01 mol) and 2-hydroxy-3-methoxybenzaldehyde (0.01 mol) were dissolved in methanol (10 ml) solvent. The mixture was refluxed on magnetic stirrer for 2–3 h. Reaction progress was monitored by TLC. After completion of reaction, the product is cooled to room temperature. The solid obtained was filtered and washed with methanol and recrystallized from aqueous ethanol (80%) to obtain pure compound (m.p. 270°C) (Scheme 1).

Synthesis of NBNCH metal complexes:

The complexes were prepared by refluxing the mixture

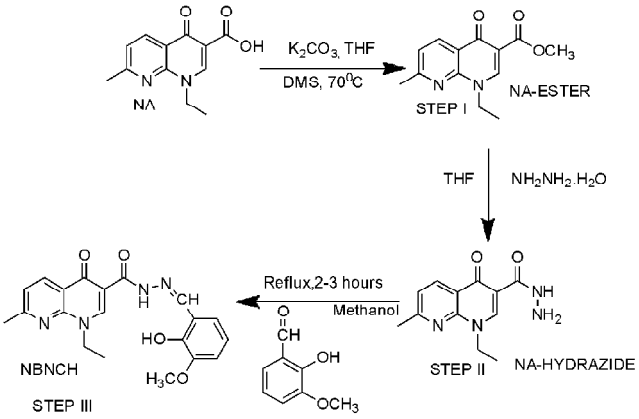

Scheme 1. Synthetic path for NBNCH.

of NBNCH in chloroform and corresponding Cu^{II}, Ni^{II} and Co^{II} metal salts in methanol (1:2 mole) for 15–20 h at 90–110°C by adjusting pH in the range 6–7 for complex formation (Scheme 2). The resulting solutions were concentrated and cooled. On cooling colored precipitate is obtained, which is filtered, washed several times with methanol, chloroform and dried. It is stored in desiccators over anhydrous $CaCl_2$. All the complexes are stable to air and moisture.

$$M.Cl_2.6HO + NBNCH \xrightarrow[CHCl_3]{\text{Methanol}} \text{NBNCH metal complexe}$$

M: Cu^{II}, Co^{II} and Ni^{II}

Scheme 2. Synthetic path for NBNCH metal complexes.

Supplementary Information

All additional information concerned to characterization of title compound (NBNCH) and it's Cu^{II}, Co^{II} and Ni^{II} complexes using various spectro-analytical techniques are compiled in Supplementary Information.

Acknowledgement

The authors are grateful to Department of Chemistry and Instrumentation Lab Facilities, Osmania University for providing necessary facilities, the Central Facilities for Research and Development (CFRD), Osmania University for providing necessary facilities. We also acknowledge the Research and Training Centre in Biotechnology, Karnataka and Sophisticated Analytical Instrument Facility (SAIF), IIT Bombay. One of the authors (NN) expresses sincere thanks to the UGC, New Delhi for financial support to carry out this work.

References

1. D. C. Hooper and J. S. Wolfson, American Society for Microbiology, 2nd ed., New York, 1993, p. 97.
2. P. Y. Shirodkar and M. VartakMeghna, *Indian J. Heterocyclic Chem.*, 2000, ***9***, 239.
3. V. K. Pandey, D. Misra and A. Shukla, *Indian Drugs*, 1994, **31**, 532.
4. N. C. Desai, B. R. Shah, J. J. Bhatt, H. H. Patel, N. K. Undavia, P. B. Trivedi and V. Narayanan, *Indian J. Chem.*, 1995, **34B**, 201.
5. L. M. Werbel, E. F. Elslager and L. S. Newton, *J. Heterocyclic Chem.,* 1987, **23**, 345.
6. N. B. Patel and J. D. Lilakar, *Indian J. Heterocyclic Chem.*, 2001, **11**, 85.
7. G. Y. Leisher, E. J. Froelich, M. D. Gruett, J. H. Bailey and P. R. Brundage, *J. Med. Pharm. Chem.*, 1962, **5**, 1063.
8. A. M. Emmerson and A. M. Jones, *Journal of Antimicrobial Chemotherapy,* 2003, **51**, 13.
9. J. E. F. (Ed.), Reynolds and Martindale, The Pharmaceutical Press, London, 1993, p. 192.
10. J. M. Shiminzu, S. Nakamura, Y. Takase and N. Kurobe, *Antimicrobial Agents and Chemotherapy*, 1975, **7**, 441.
11. W. A. Gross, W. H. Deitz and T. M. Cook, *J. Bacteriol.*, 1964, **88**, 1112.
12. T. M. Cook, K. G. Brown, J. V. Boyle and W. A. Gross, *J. Bacteriol.*, 1964, **92**, 1510.
13. A. M. Kamel, M. A. Lobna, M. L. El-Sayed, I. H. Mohamed and H. B. Raina, *Bio. Med. Chem.,* 2006, **14**, 8675.
14. A. Ozdemir, G. Turan-zitouni, Z. A. Kaplancikl and G. Iscan, *Med. Chem.*, 2008, **23**, 470.
15. J. R. Dimmock, S. C. Vashisha and J. P. Stables, *Eur. J. Med. Chem.*, 2000, **35**, 241.
16. R. Kalsi, M. Shrimali, T. N. Bhalla and J. P. Barthwal, *Indian J. Pharm. Sci.,* 2006, **41**, 353.
17. P. Melnyk, V. Leroux Sergheraert and P. Grellier, *Bioorg. Med. Chem. Lett.*, 2006, **16**, 31.
18. J. Patole, U. Sandbhor, S. Padhye, D. N. Deobagkar, C. E. Anson and A. Powell, *Bioorg. Med. Chem. Lett.,* 2003, **13**, 51.
19. H. I. Tomokazu, A. O. Nobuharu, H. K. Hiroshi, K. K. Atsushi, "Hydrazone derivatives, processes for production thereof, and uses thereof", U.S. Patent 5304573, 1994.
20. S. Norrihan, M. D. Abu Affan, M. D. Abdus Salam, F. B. Ahmad and M. R. Asaruddin, *Open Journal of Inorganic Chemistry*, 2012, **2**, 22.
21. P. Ranjithreddy, M. D. Jaheer, N. Narsimha and Ch. Sarala Devi, *Journal of Materials Science and Chemical Engineering*, 2015, **3**, 45.
22. M. D. Jaheer, P. Ranjith Reddy, N. Narsimha, P. Sujitha, B. Srinivas and Ch. Sarala Devi, *Journal of Applied Chemistry*, 2014, **7**, 1.
23. P. Vinod Singh, *Spectrochimica Acta*, 2008, **71**, 17.
24. T. F. Yen, "Electron spin resonance of metal complexes", 1st ed., Plenum Press, New York, 1969, 143.
25. K. Sudeepa, B. Aparna, M. Ravi, P. Ranjith Reddy, K. Karunakar Rao and Ch. Sarala Devi, *Journal of Research in Pharmacy and Chemistry*, 2015, **5(4)**, 668.
26. A. Rambabu, M. Pradeep Kumar, S. Tejaswi, V. Vamsikrishna and Shivaraj, *Journal of Photochemistry & Photobiology, B: Biology*, 2016, **165**, 147.
27. M. Ravi, C. H. Kishan Prasad, B. Ushaiah, E. Ravi Kumar, P. Shyam and Ch. Sarala Devi, *Journal of Fluorescence,* 2015, **25**, 1279.
28. C. H. Kishan Prasad, M. Ravi, B. Ushaiah, V. Srinu, E. Ravi Kumar and Ch. Sarala Devi, *Journal of Fluorescence*, 2016, **26**, 189.
29. N. Narsimha, K. Sudeepa, M. D. Jaheer, M. Ravi, Sreekanth Sivan and Ch. Sarala Devi, *Journal of Fluorescence,* 2018, **28**, 225.
30. N. Narsimha, P. Ranjith Reddy, M. D. Jaheer, B. Aparna and Ch. Sarala Devi, *International Journal of Research in Pharmacy and Chemistry,* 2015, **5**, 615.